Supporting Information

Nanotubes Embedded Indocyanine Green-Hyaluronic Acid Nanoparticle for Photoacoustic Imaging Guided Phototherapy

Guohao Wang[1], Fan Zhang[1], Rui Tian[2,], Liwen Zhang[1], Guifeng Fu[1], Lily Yang[3] and Lei Zhu[1,3,*]*

1. State Key Laboratory of Molecular Vaccinology and Molecular Diagnostics & Center for Molecular Imaging and Translational Medicine, School of Public Health, Xiamen University, Xiamen, Fujian, 361005, China;
2. Department of Ophthalmology Second Hospital, Jilin University, Changchun, Jilin, 130033, China;
3. Departments of Surgery and Radiology and Imaging Sciences, Emory University School of Medicine, Atlanta, Georgia 30322, United States.

Corresponding Author

* To whom correspondence should be addressed. Tel: (+)86-592-2880642, Fax: (+)86-592-2880642; E-mail: lei.zhu@xmu.edu.cn (L.Z.) and 18604303265@163.com (R.T.)

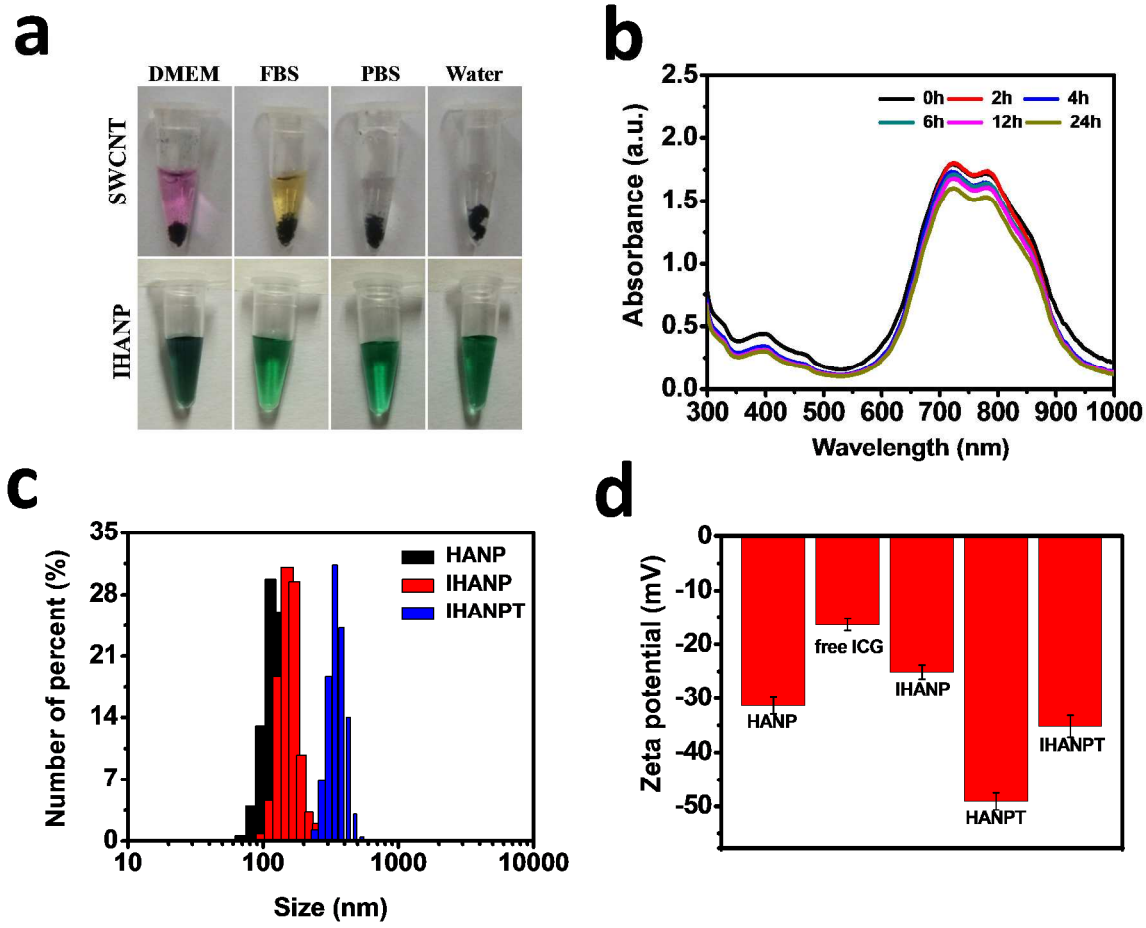

Figure S1. (a) Stability of SWCNT and IHANP in water, PBS, fetal bovine serum (FBS) and cell medium after 2 weeks. (b). UV-vis-NIR spectrum of IHANP in fetal bovine serum for 24 h. (c). Dynamic light scattering analysis for the particle size distribution of HANP (177 ± 9.5 nm), IHANP (195 ± 12 nm) and IHANPT (389 ± 23 nm). (d). Zeta potential of IHANPT, HANPT, IHANP, ICG and HANP.

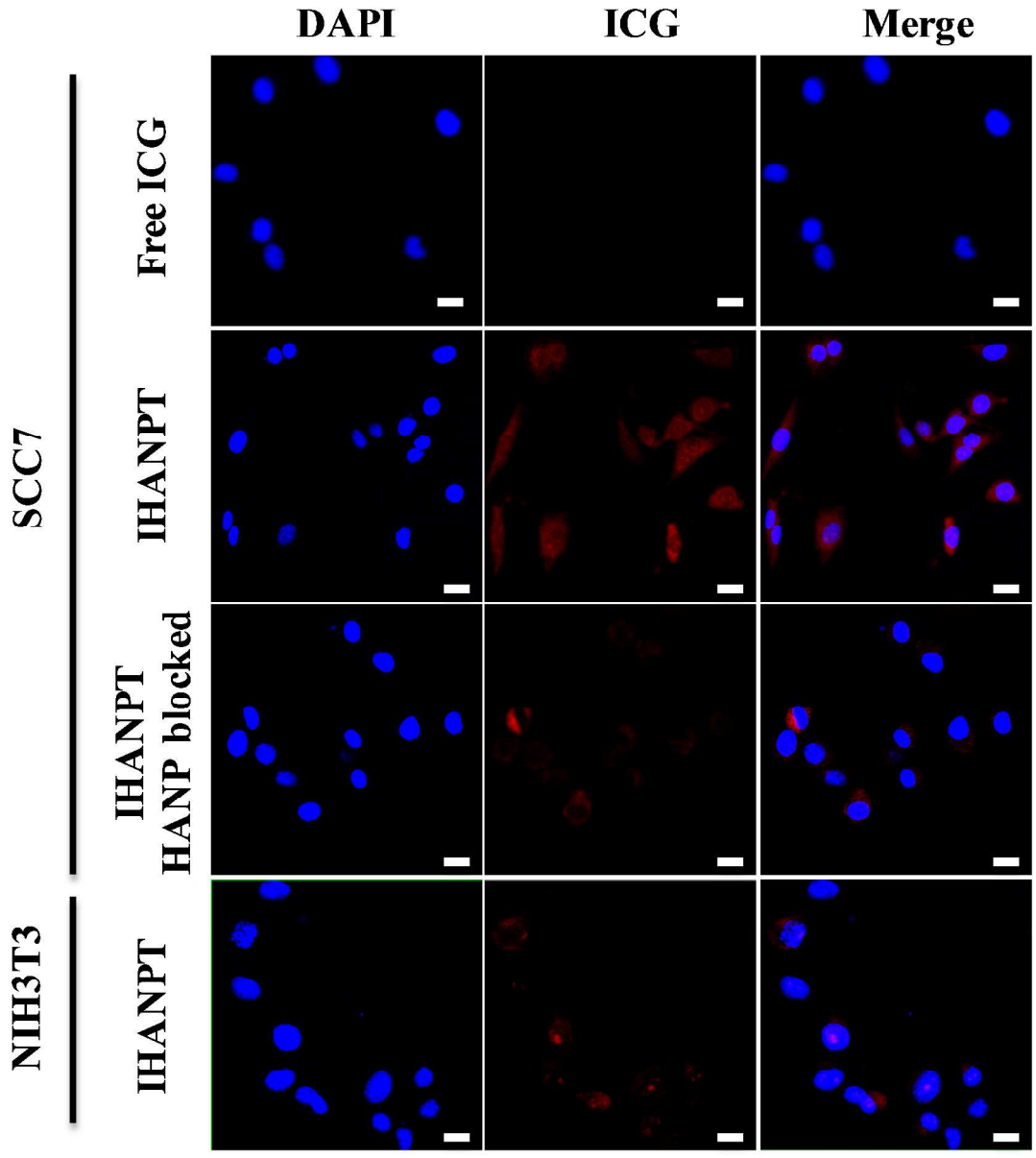

Figure S2. Tumor targetability of IHANPT. *In vitro* fluorescence staining of CD44 positive (SCC7) and negative (3T3) cells. 1 μM IHANP was used for cell labeling10 μM of HANP was used for blocking test. Red color is from ICG for CD44 and blue color is from DAPI for nuclei visualization (Scale bar = 20 μm).

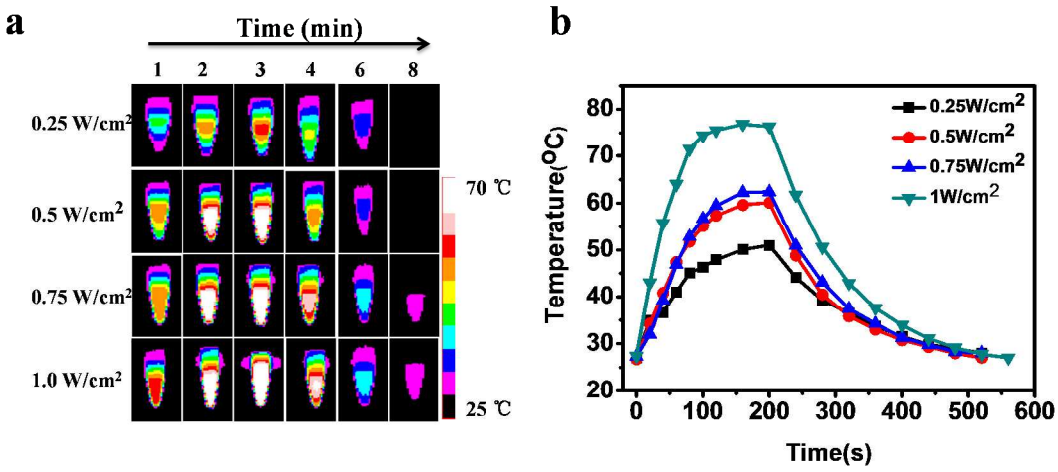

Figure S3. Characterization of free ICG. (a) Infrared thermographic maps of centrifuge tubes with free ICG, was measured with an infrared thermal imaging camera after different intensities of laser irradiation. (b) Maximum temperature profiles of free ICG, as a function of the irradiation time under continuous laser irradiation at a diverse intensity.

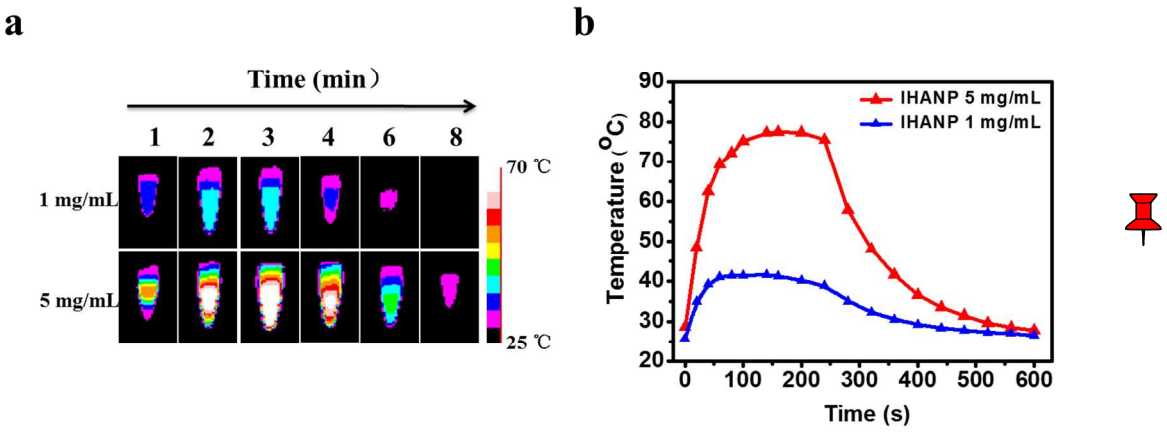

Figure S4. Characterization of IHANPT. (a) Infrared thermographic maps of centrifuge tubes with IHANPT, was measured with an infrared thermal imaging camera under continuous laser irradiation at a power intensity of 0.3 W/cm^2. (b) Maximum temperature profiles of IHANPT, as a function of the irradiation time under continuous laser irradiation at a power intensity of 0.3 W/cm^2.

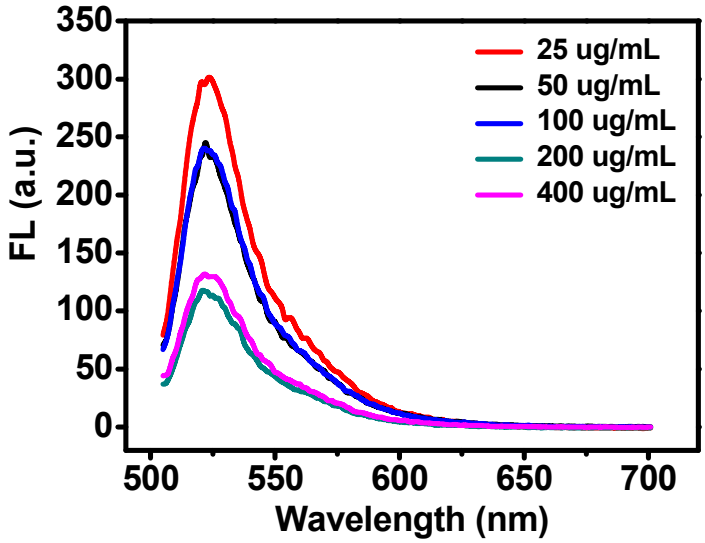

Figure S5. The FL spectra of $^1O_2$ sensor Free ICG at different concentration with laser irradiation for 10 min (808 nm laser, light dose rate: 0.3W/cm^2).

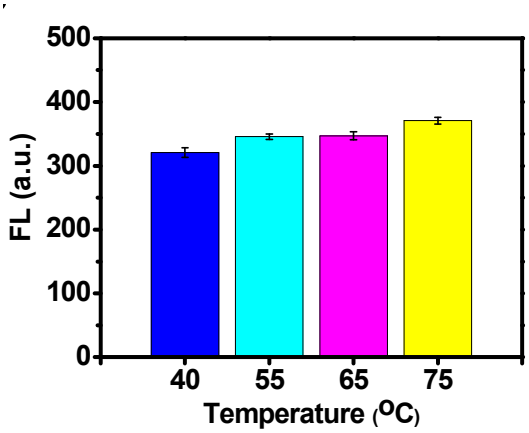

Figure S6. Quantification of DCF fluorescent intensity at different temperatures. The fluorescence intensity of DCF produced from DCFH incubation with H_2O_2 at different temperatures. No significant fluorescent changes were found, suggesting the minimum influence of temperature on DCF signals.

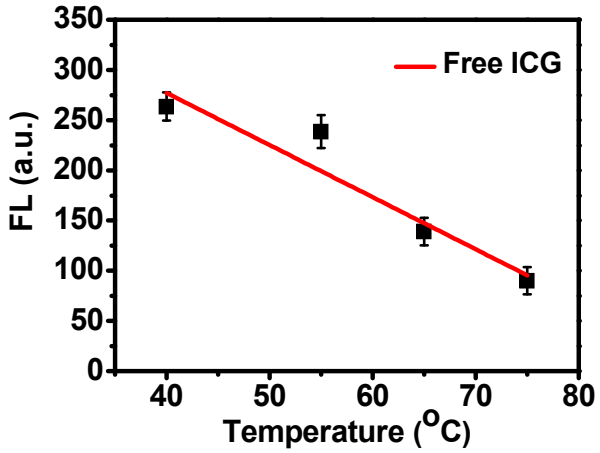

Figure S7. The effects of temperature on the production of $^1O_2$ of free ICG.

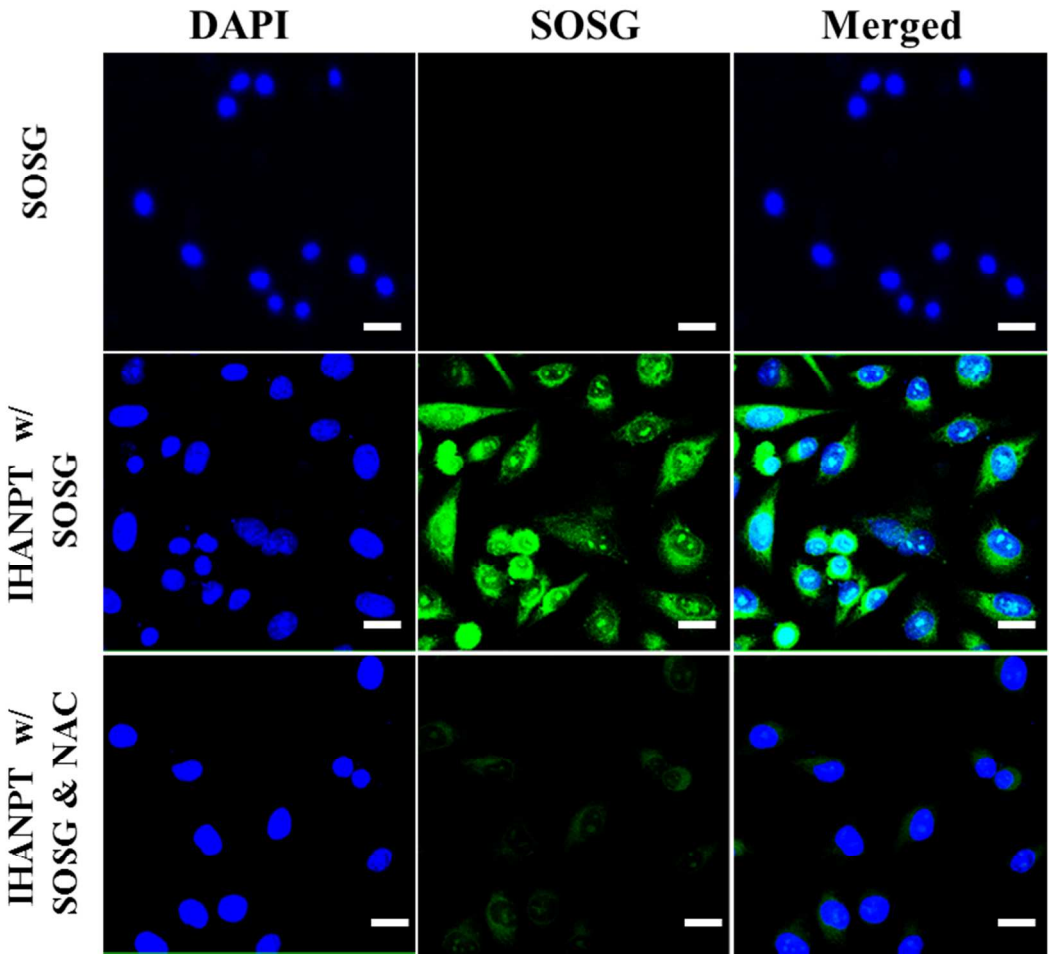

Figure S8. The $^1O_2$ production within cells was examined by confocal fluorescence imaging. Confocal fluorescence images of SCC7 cells with different treatments after 808 nm irradiation: SOSG only, IHANPT NPs + SOSG, and NAC + IHANPT NPs + SOSG. The scale bar equals to 20 μm.

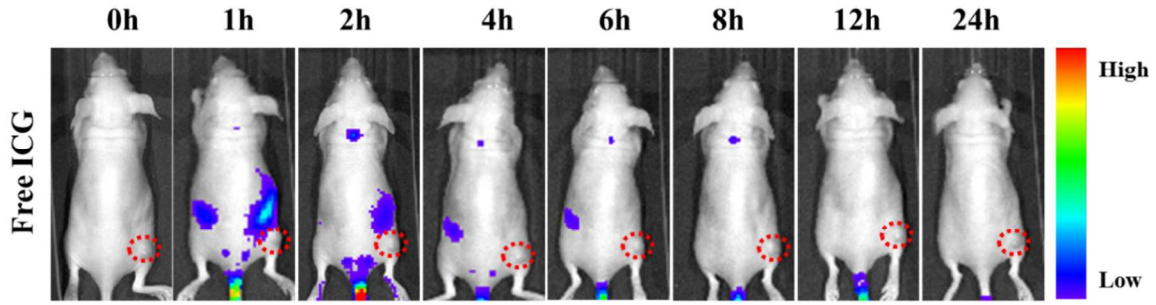

Figure S9. *In vivo* FL imaging of nude mice bearing 4T1 tumors after i.v. injection of free ICG at different time points.

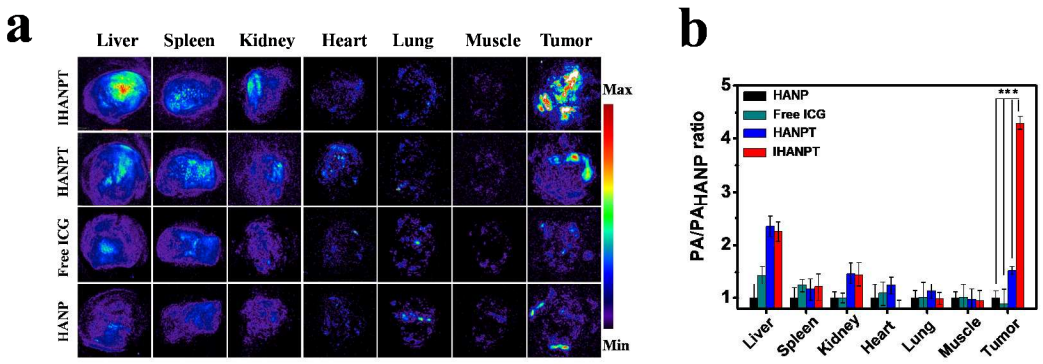

Figure S10. Biodistribution analysis of IHANPT, IHANPT, ICG, HANP by photoacoustic tomography imaging (PA). (a) *Ex vivo* PA of major organs and tumors excised at 24 h post-injection. (b) Quantification of PA signal changes of each organ and tumor. Compared with PA signals of HANP, the increased fold of PA signals at indicated time points were calculated. Error bars represent the standard deviations of 3 mice per group. *, $P<0.05$.

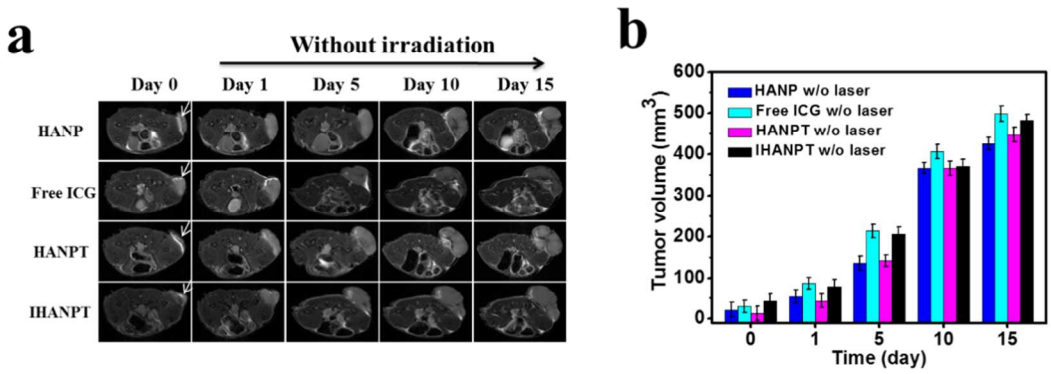

Figure S11. MRI monitoring the therapy response of IHANPT. (a) After different treatment without laser, MR imaging was employed to monitor the therapeutic responses.(b) The total tumor volume of different groups of SCC7 tumor-bearing mice determined by T2WI MRI after indicated treatments without laser.